JOURNAL OF MATERIALS SCIENCE 19 (1984) 672–682

Fracture of ceramics with surface flaws introduced by Knoop indentation

T. FETT
Kernforschungszentrum Karlsruhe, Arbeitsgruppe Zuverlässigkeit und Schadenskunde am Institut für Reaktorbauelemente, West Germany

The crack opening behaviour of surface flaws in ceramic materials, produced by Knoop indentation tests, was investigated. The damaged region below the indenter tip was replaced by a wedge. The influence of this wedge is reduced, if tensile stresses are acting at the damaged surface. For alumina the wedging force in moment of fracture was found approximately 50% of its value without additional bending.

1. Introduction

In the last 10 years indentation fracture mechanics has been developed for ceramic materials [1–10]. The sizes of surface flaws, produced by indentation tests, have been evaluated for a simple determination of K_c-values. On the other hand such well defined damaged surfaces are ideal specimens for fracture mechanical investigations.

During the indentation of a Knoop diamond under load F into the surface of a ceramic material, a semi-elliptic crack with radius R extends (Fig. 1). The indented region of depth a' and length $2b'$ is greatly damaged and plastically deformed. For computations this region shall be replaced by a semicircle with an effective radius a where $a' < a < b'$.

The damaged region acts as a plain wedge and keeps the crack open. Thus a tensile stress field results in the vicinity of the crack tip and may influence the strength behaviour. In bending tests the strength is found to be lower than expected from crack sizes and fracture toughness K_c. This indicates, that the effect of the "wedge" will not vanish and the crack will not open before failure occurs. In practice, this effect can be avoided by annealing or grinding off this damaged zone.

A detailed analysis of the opening behaviour of such cracks is made in this work.

2. Crack opening behaviour of Knoop indentation flaws

The theoretical considerations are based on a penny-shaped crack in an infinite body, which is opened by a circular wedge of the thickness $2\delta(0)$ in its centre (Fig. 2). The case of a Knoop indentation flaw is approximated by cutting the infinite body through the crack centre. Surface effects shall be neglected. In Fig. 2, the following symbols are used: R is the crack radius; r is the distance from crack centre; a is the wedge radius; and δ is the crack opening displacement. Dimensionless radii are $c = a/R$ and $\rho = r/R$.

Under a condition of axial symmetry, the stresses σ and the crack opening displacements δ can be calculated by Hankel-transformations and solving a system of integral equations. It results in [11, 12]

$$\delta(\rho) = \frac{4R}{\pi E'} \int_\rho^1 \frac{g(x)\,\mathrm{d}x}{(x^2-\rho^2)^{1/2}}$$
$$g(x) = \int_0^x \frac{p(\rho)\,\rho\,\mathrm{d}\rho}{(x^2-\rho^2)^{1/2}} \qquad (1)$$

with $E' = E/(1-\nu^2)$ where ν is Poisson's ratio, E is Young's modulus, and $p(\rho)$ is the pressure distribution.

2.1. Crack opening at constant wedge pressure

2.1.1. General solution

In case of partially constant pressure distribution

$$\text{(I)} \qquad p(\rho) = \begin{cases} p_0 & \text{for } 0 \leqslant \rho < c \\ 0 & \text{for } c < \rho < 1 \end{cases}$$

one obtains from Equation 1 for $x \leqslant c$

$$g_1(x) = p_0 \int_0^x \frac{\rho\,\mathrm{d}\rho}{(x^2-\rho^2)^{1/2}} = p_0 x \qquad (2)$$

0022–2461/84 $03.00 + .12

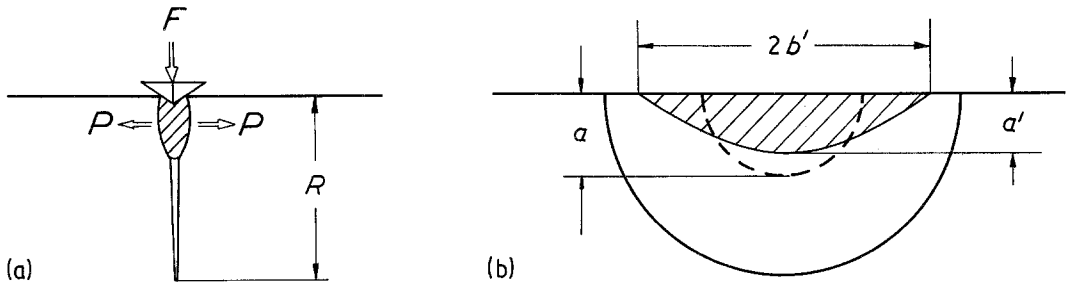

Figure 1 Generation of surface crack by a Knoop indentation test.

and for $x > c$

$$g_2(x) = p_0 \int_0^c \frac{\rho \mathrm{d}\rho}{(x^2-\rho^2)^{1/2}} = p_0[x-(x^2-c^2)^{1/2}] \tag{3}$$

The crack opening displacement $\delta'_p(\rho, c)$ normalized on R and p_0 is introduced by

$$\delta'_p(\rho, c) = \frac{\pi E'}{4Rp_0}\delta(\rho, c)$$

Index p in δ'_p means p = constant in the wedge, i.e. a plastically deformable wedge. From Equation 1 one obtains

$$\delta'_p(\rho, c) = \int_\rho^c \frac{x\mathrm{d}x}{(x^2-\rho^2)^{1/2}} + \int_c^1 \frac{x-(x^2-c^2)^{1/2}}{(x^2-\rho^2)^{1/2}}\mathrm{d}x$$

$$= \int_\rho^1 \frac{x\mathrm{d}x}{(x^2-\rho^2)^{1/2}} - \int_c^1 \left(\frac{x^2-c^2}{x^2-\rho^2}\right)^{1/2}\mathrm{d}x \tag{4}$$

$$\delta'_p(\rho, c) = (1-\rho^2)^{1/2}[1-(1-c^2)^{1/2}] + c[\mathbb{E}(\rho, c) - E(\arcsin c, \rho/c)] \quad \text{for } \rho \leqslant c$$

and

$$\delta'_p(\rho, c) = \int_\rho^1 \frac{x-(x^2-c^2)^{1/2}}{(x^2-\rho^2)^{1/2}}\mathrm{d}x$$

$$= (1-\rho^2)^{1/2}[1-(1-c^2)^{1/2}] + \rho[\mathbb{E}(c/\rho) - (1-c^2/\rho^2)\mathbb{K}(c/\rho) - E(\arcsin\rho, c/\rho) + (1-c^2/\rho^2)F(\arcsin\rho, c/\rho)] \quad \text{for } \rho > c \tag{5}$$

$F(\phi, k)$, $E(\phi, k)$ are the incomplete elliptical integrals for the first and second kinds and $\mathbb{K}(k)$, $\mathbb{E}(k)$ the related complete elliptical integrals.

Fig. 3 is a representation of Equations 4 and 5 for $c = 0.2$. In special cases the general Equations 4 and 5 can be replaced by elementary functions. The maximum value of displacement occurs at $\rho = 0$. From Equation 4 results

$$\delta'_p(0, c) = \int_0^c \mathrm{d}x + \int_c^1 [1-(1-(c/x)^2)^{1/2}]\,\mathrm{d}x$$

$$= 1-(1-c^2)^{1/2} + c\arccos c \tag{6}$$

If a constant pressure p acts over the whole crack area, i.e. $c = 1$, we get

$$\delta'_p(\rho, 1) = (1-\rho^2)^{1/2} \tag{7}$$

2.1.2. Stress-intensity factor

In case of an axially symmetric stress distribution, the stress-intensity factor is

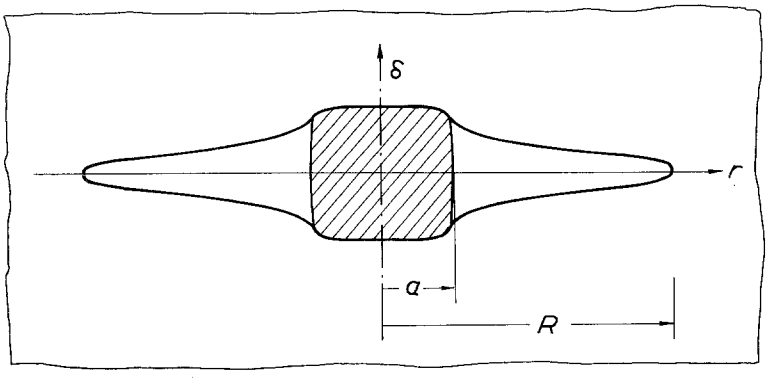

Figure 2 Cross-section of a wedged penny-shaped crack in an infinite body.

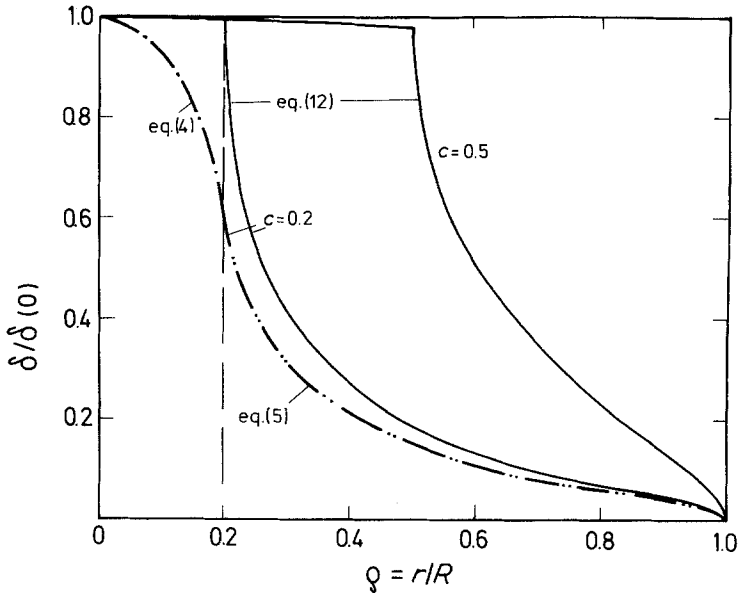

Figure 3 Crack opening profiles of a different wedged penny-shaped crack.

$$K_p = \frac{2}{(\pi R)^{1/2}} \int_0^R \frac{p(r) r \mathrm{d}r}{(R^2 - r^2)^{1/2}} \qquad (8)$$

A pressure distribution

$$p(r) = \begin{cases} p_0 & \text{for } 0 \leqslant r \leqslant a \\ 0 & \text{for } a < r < R \end{cases}$$

leads to

$$K_p = \frac{2}{(\pi R)^{1/2}} p_0 \int_0^a \frac{r \mathrm{d}r}{(R^2 - r^2)^{1/2}} = \frac{2 p_0 R^{1/2}}{\pi^{1/2}} \{1 - [1 - (a/R)^2]^{1/2}\} \qquad (9)$$

If the pressure is concentrated in the centre of the crack as a pair of forces $\pm P$ we obtain, with $[1 - (a/R)^2]^{1/2} \to 1 - \frac{1}{2}(a/R)^2$

$$K = \frac{P}{(\pi R)^{3/2}} \quad \text{with} \quad P = p_0 a^2 \pi \qquad (10)$$

2.2. Crack opening behaviour for a rigid wedge

In case of a rigid plain wedge the problem is described by

$$\delta(\rho) = \delta(0) \quad \text{for } 0 \leqslant \rho \leqslant c$$

$$p(\rho) = 0 \quad \text{for } c < \rho < 1$$

$$\delta(\rho) = 0 \quad \text{for } \rho > 1$$

This mixed boundary value problem requires the solution of a system of three simultaneous integral equations.

2.2.1. Approximation for pressure distribution

A simple approximation of the given crack opening problem is based on the well known problem of elasticity, the impression of a rigid rod into the plain surface of an elastical material [13]. For the pressure distribution in the rigid wedge we assume

$$p(\rho) \simeq \begin{cases} p(0)/[1 - (\rho/c)^2]^{1/2} = p(0) \dfrac{a}{(a^2 - r^2)^{1/2}} & \text{for } \rho \leqslant c;\ r \leqslant a \\ 0 & \text{for } \rho > c;\ r > a \end{cases} \qquad (11)$$

The associated crack opening displacement defined by

$$\delta_r'(\rho, c) = \frac{\pi E'}{4 R p(0) c} \delta_r(\rho, c)$$

index r meaning rigid, is obtained from Equations 1 and 2

$$2\delta_r'(\rho, c) \simeq \int_\rho^c \frac{\ln [(c + x)/(c - x)]}{(x^2 - \rho^2)^{1/2}} \mathrm{d}x + \int_c^1 \frac{\ln [(x + c)/(x - c)]}{(x^2 - \rho^2)^{1/2}} \mathrm{d}x \qquad (12)$$

The displacement at $\rho = 0$ is then given by

$$2\delta'_r(0,c) \cong \int_0^c \frac{1}{x}\ln\left(\frac{c+x}{c-x}\right)dx + \int_c^1 \frac{1}{x}\ln\left(\frac{x+c}{x-c}\right)dx = 2[L_2(1)-L_2(-1)]-[L_2(c)-L_2(-c)] \quad (13)$$

where the Euler dilogarithm $L_2(x)$ is defined by [14]

$$L_2(x) = \sum_{\nu=1}^{\infty} \frac{x^\nu}{\nu^2}$$

The displacement, calculated from Equation 12 is represented in Fig. 3 for $c = 0.2$ and $c = 0.5$.

2.2.2. Stress-intensity factor

From Equation 8 and the approximated pressure distribution Equation 11 the stress-intensity factor K_r follows as

$$K_r \simeq \frac{2}{(\pi R)^{1/2}}\int_0^R \frac{rp(r)dr}{(R^2-r^2)^{1/2}} = \frac{2p(0)a}{(\pi R)^{1/2}}\int_0^a \frac{rdr}{(R^2-r^2)^{1/2}(a^2-r^2)^{1/2}} \quad (14)$$

with the solution [14]

$$K_r \simeq \frac{p(0)a}{(\pi R)^{1/2}}\ln\left(\frac{R+a}{R-a}\right) = p(0)\left(\frac{R}{\pi}\right)^{1/2} c\ln\left(\frac{1+c}{1-c}\right) \quad (15)$$

In the literature on indentation tests the representation of stress-intensity factors is given in quantities of acting forces. In the case of a wedge with constant pressure, Equation 10 results. In case of a rigid wedge one obtains because of

$$\ln\left(\frac{1+c}{1-c}\right) = 2\,\text{artanh}\,c \simeq 2c \quad (16)$$

the expression

$$K_r \simeq \frac{2p(0)a^2}{\pi^{1/2}R^{3/2}} \quad (17)$$

The wedge force is obtained by integration of the pressure distribution

$$P = 2\pi p(0)a\int_0^a \frac{rdr}{(a^2-r^2)^{1/2}} = 2\pi p(0)a^2 \quad (18)$$

and thus

$$K_r = \frac{P}{(\pi R)^{3/2}} \quad (19)$$

i.e. identical to Equation 10.

Between the wedge forces P and the Knoop indentation load F (Fig. 1) a simple relationship

$$P = \chi F/\pi^{3/2} \quad (20)$$

can be assumed, where χ includes the geometry of the Knoop indenter. So the well known formula results [15–22]

$$K_F = \chi\frac{F}{R^{3/2}} \quad (21)$$

The crack opening displacement at the surface $\delta(\rho = 0)$ can be expressed by appropriate stress-intensity factors. A combination of Equations 6, 9, 13 and 15 yields

$$\frac{\delta(0)}{K} = \frac{2}{E}\frac{R^{3/2}}{\pi^{1/2}a}g(a/R) \quad (22)$$

with

$$g(c) = \begin{cases} c + \dfrac{c^2 \arccos c}{1-(1-c^2)^{1/2}} & \text{for plastical wedge} \\ \dfrac{L_2(1)-L_2(-1)-\frac{1}{2}[L_2(c)-L_2(-c)]}{\frac{1}{2}\ln[(1+c)/(1-c)]}\,c & \text{for rigid wedge} \end{cases} \quad (23)$$

The functions $g(c)$ are represented in Fig. 4.

For numerical computations it is useful to employ an averaged formula

$$g(c) \simeq c + \frac{c^2 \arccos c}{1-(1-c^2)^{1/2}} - 0.35 \quad (24)$$

which is also shown in Fig. 4. From Equation 21 and Equation 22 we get

$$\delta(0) = \frac{2}{\pi^{1/2}}\frac{\chi}{Ea}Fg(a/R) \quad (25)$$

If the crack is not loaded by a wedge but by a uniform tensile stress σ we find

$$\frac{\delta(0)}{K} = \frac{2}{\pi^{1/2}}\frac{R^{1/2}}{E} \quad \text{with} \quad K = \frac{2\sigma R^{1/2}}{\pi^{1/2}} \quad (26)$$

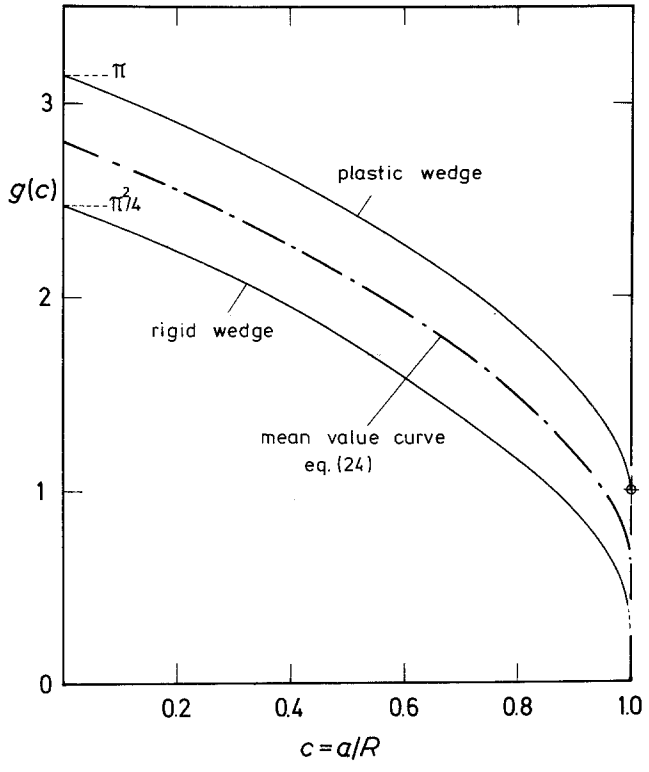

Figure 4 Representation of $g(c)$ for a plastic and a rigid wedge.

3. Knoop indentation tests

In the following the case of an indentation test in a surface which contains residual surface stresses σ_r is analysed. The size of the penny-shaped crack is governed by

$$\frac{\chi F}{R^{3/2}} + \sigma_r Y R^{1/2} = K_c \qquad (27)$$

In case of a previously annealed specimen we obtain, because of $\sigma_r = 0$, a different crack size R_0

$$\chi F/R_0^{3/2} = K_c \qquad (28)$$

Introduction of

$$\sigma_c = K_c/Y(R_0)^{1/2} \qquad (29)$$

and combination of Equations 27 and 28 lead to

$$(R_0/R)^{3/2} + \frac{\sigma_r}{\sigma_c}(R/R_0)^{1/2} = 1$$

and finally to

$$(R_0/R)^2 - (R_0/R)^{1/2} = -\sigma_r/\sigma_c \qquad (30)$$

3.1. Residual wedging after indentation test

If δ_0 is the thickness of the wedge produced during the indentation test and δ_1 is the thickness after removal of the indentation force, the ratio of both values is described by

$$\delta_1 = \alpha\delta_0 \quad 0 \leqslant \alpha \leqslant 1 \qquad (31)$$

where the factor α is assumed to be constant for a given fixed force F. Between the crack opening displacements, caused by the wedge force F and residual surface stresses σ_r, and the wedge thickness, the relation

$$\delta_0 = \delta(K_F) + \delta(K_{\sigma r}) \qquad (32)$$

with $\delta(K_F)$ from Equation 22 and $\delta(K_{\sigma r})$ from Equation 26, must be satisfied. After removal of the indenter an additional stress σ shall be applied – for instance in a bending test – so that instead of σ_r a new surface stress $\sigma_a = \sigma + \sigma_r$ will act. Since stable crack growth may occur under these stress conditions a different crack radius R^* may appear.

In analogy to Equation 32, one obtains from Equation 31

$$\delta_1 = \delta(K_F^*) + \delta(K_{\sigma a}^*) = \alpha[\delta(K_F) + \delta(K_{\sigma r})] \quad \delta(K_F^*) \geqslant 0 \qquad (33)$$

where

$$K_F^* = \chi F'/R^{*3/2} \quad K_{\sigma a}^* = \sigma_a Y(R^*)^{1/2}$$

and F' is the residual wedge force.

The stress-intensity factor K_F^*, caused by residual wedging, can be calculated from Equations

22, 26 and 21 as

$$K_F^* = \alpha \left[\left(\frac{R}{R^*}\right)^{3/2} \frac{g(c)}{g(c^*)} K_F + \left(\frac{R}{R^*}\right)^{1/2} \frac{c^*}{g(c^*)} K_{\sigma r} \right] - \frac{c^*}{g(c^*)} K_{\sigma a}^* \quad (34a)$$

where $c^* = a/R^*$.

Since during indentation

$$K_F + K_\sigma = K_c \quad (35)$$

is fulfilled, Equation 34a becomes

$$K_F^* = \frac{\alpha}{g(c^*)} \left(\frac{R}{R^*}\right)^{3/2} [g(c)K_c - (g(c) - c)K_{\sigma r}] - \frac{c^*}{g(c^*)} K_{\sigma a}^* \quad (34b)$$

If we introduce the forces, F, F' and stresses σ_r, σ_a, it follows from Equation 34

$$\chi F' = \frac{\alpha}{g(c^*)} [\chi F g(c) + aYR\sigma_r] - \frac{a}{g(c^*)} YR^*\sigma_a \quad (36)$$

where $Y = 2/\pi^{1/2}$.

It is evident from Equation 34, that the influence of residual wedging will decrease with increasing tensile stresses applied (σ_a, $K_{\sigma a}^*$), i.e. the wedge will become more and more unloaded. The condition for total unloading, when the crack surfaces move away the wedge is given by $K_F^* = 0$.

The influence of residual wedging on the strength behaviour of Knoop damaged specimens can be sufficiently described by Equation 34. The unknown parameters α and a must be determined from strength tests. In these tests it will be attempted to verify Equation 34, i.e. to verify the simple assumption, that $\alpha =$ constant for $F =$ constant.

4. Computation of bending strength

If the Knoop indentation test is performed on a specimen free of stress, Equation 34 furnishes the results $K_{\sigma r} = 0$; $R = R_0$, i.e. $c = c_0 = a/R_0$. The residual wedging after removal of the load becomes

$$K_F^* = \alpha K_c$$

A bending test will be made with this damaged specimen so that the surface flaw is placed in the tensile region. Taking into account that stable crack growth may occur, Equation 34 gives

$$K_F^* = \alpha \frac{g(c_0)}{g(c^*)} \left(\frac{R_0}{R^*}\right)^{3/2} K_c - \frac{c^*}{g(c^*)} K_{\sigma a}^* \quad (37)$$

with

$$K_{\sigma a}^* = \sigma_a Y (R^*)^{1/2}$$

The total stress-intensity factor during the bending test is

$$K_{tot} = K_F^* + K_{\sigma a}^* \quad (38)$$

A stable crack growth, starting from the original crack size R_0, will occur if K_{tot} decreases with increasing R, i.e.

$$\left.\frac{\partial K_{tot}}{\partial R^*}\right|_{R^*=R_0} < 0 \quad K_{tot}|_{R^*=R_0} = K_c$$

The crack extends up to a critical value of R^*, named R_c, at which spontaneous failure takes place. At that moment the conditions

$$\left.\frac{\partial K_{tot}}{\partial R^*}\right|_{R^*=R_c} \geqslant 0 \quad (39)$$

and

$$K_{tot}|_{R^*=R_c} = K_c \quad (40)$$

must be satisfied. In this case the Conditions 39, 40 lead to an equilibrium crack size

$$R_c \leqslant R_0$$

no stable crack growth can occur and the catastrophical crack extension will start from the crack contour produced by the indentation test. Then the total stress-intensity factor is given by

$$K_{tot} = \alpha K_c + K_{\sigma a}[1 - c_0/g(c_0)] \quad (41)$$

$$K_{\sigma a} = \sigma_a Y (R_0)^{1/2}$$

So one obtains the bending strength with regard to Equation 29

$$\sigma_B = \frac{1 - \alpha}{1 - c_0/g(c_0)} \sigma_c \quad (42)$$

The results of computations with Equations 39, 40 and 42 are indicated in Fig. 5; the bending strength σ_B is normalized to σ_c. σ_c represents the strength of the Knoop damaged specimen in the absence of wedging forces. Below the dash-dotted line the calculation of σ_B leads to critical crack sizes $R_c > R_0$. The strength above this line is obtained from Equation 42.

This relation $\sigma_B/\sigma_c = f(\alpha, c_0)$ allows to eliminate one of the unknown parameters α, c_0 in Equation 34 by measurent of σ_B and σ_c.

4.1. Bending tests with Knoop-damaged specimen

For the determination of σ_c the stresses in the vicinity of the crack tip, caused by interaction

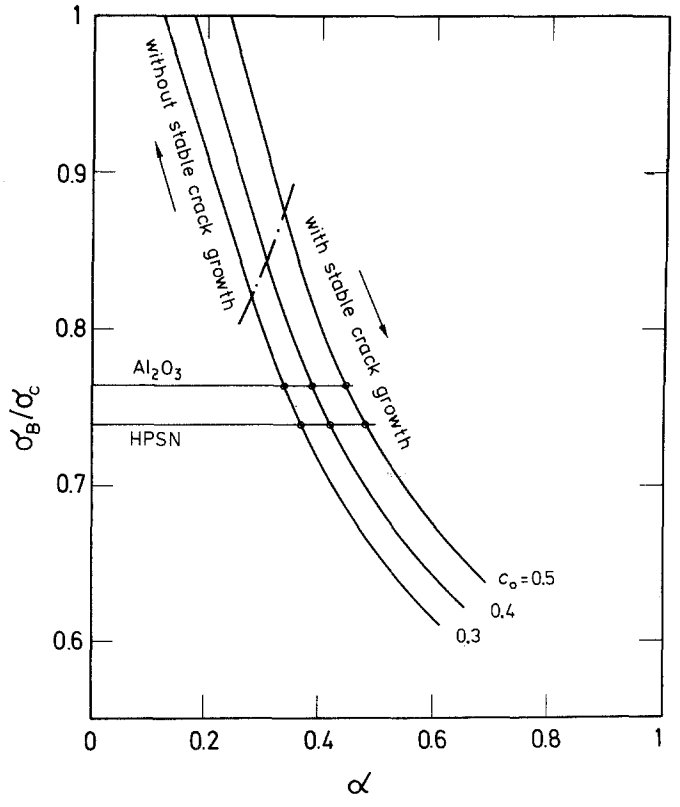

Figure 5 Bending strength σ_B of a Knoop damaged specimen, normalized to σ_c, as a function of α and c_0, calculated from Equations 34, 38, 39, 40 and 42.

between the wedge and crack surface, must be annealed. Therefore, strength measurements in 4-point-bending tests were done after annealing at different temperatures. First specimens of 5 mm x 4.5 mm x 45 mm (Al_2O_3) and 3.5 mm x 4.5 mm x 45 mm (HPSN) were annealed for 4 h at 1150° C in the vacuum to remove the residual stresses created during fabrication of the specimen. These specimens were "controlled" damaged by Knoop indentation tests with an indentation load $F = 100$ N for Al_2O_3 and 160 N for HPSN and than annealed at different temperature. Since crack healing can occur at high temperatures [10, 23] annealing was performed in a vacuum of 10^{-5} torr. After an annealing duration of 4 h the temperature was reduced in steps of 200° C and with 30 min thermal retardation.

The bending strength at 0.5 mm min^{-1} cross-head speed is shown in Fig. 6 and Fig. 7. It can be seen from Fig. 6 that the residual stresses in Al_2O_3 are removed at temperatures above 1000° C. All tested specimens failed at the points of indentation. So crack-healing can be excluded. Indications of a crack tip blunting in addition to the desired stress relaxation were not found. Measurements on HPSN are shown in Fig. 7. In this material viscous flow near the crack tip cannot be excluded. This is suggested by the dependence of fracture toughness [24] on the temperature. An indication is therefore the reduction of bending strength scatter at 1300 and 1400° C. A separation of both effects is certainly not easy.

The decrease in strength at high temperatures can be caused by a change in structure or by subcritical crack growth, since crack tip stresses will not vanish instantly. From the measurements on Al_2O_3 one obtains

$$\sigma_B/\sigma_c = 0.764$$

This value is shown in Fig. 5. So the relation $\alpha = f(c_0)$ is known for this material. From the strength tests on HPSN it results with the assumption that all changes in strength are caused by annealed stresses

$$\sigma_B/\sigma_c = 0.740$$

5. Indentation tests on prestressed specimens

In addition to the indentation tests on specimens free of stress, measurements were performed on controlled prestressed ceramic surfaces. Compressive surface stresses can be produced in a 3-point-bending test [19, 25] as shown in Fig. 8.

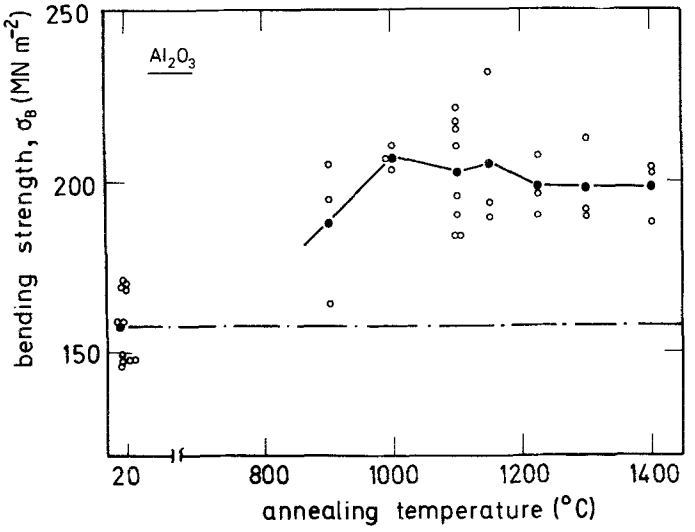

Figure 6 Bending strength of Knoop damaged specimen after 4 h annealing time at various annealing temperatures.

The indenter produces a surface crack and because of 3-point-bending a compressive surface stress at the point of indentation. By changing the roller distance, different stresses can be caused with the same indenter load.

The bending strength of such damaged specimen (crack in tension) can be computed with Equations 39, 40, but instead of Equation 37 we have to apply Equation 34. If $R_c < R$, R being taken from Equation 30, the calculation must be made with

$$\sigma_B/\sigma_c = \frac{1-\alpha}{1-\frac{c_0}{g}\frac{R_0}{R}}(R_0/R)^{1/2} - \frac{\alpha - \frac{c_0}{g}\frac{R_0}{R}}{1-\frac{c_0}{g}\frac{R_0}{R}} \times [(R_0/R)^2 - (R_0/R)^{1/2}] \quad (43)$$

$$g = g(c_0 R_0/R)$$

The bending strengths, calculated with freely chosen values of c_0, are shown in Fig. 9 for Al_2O_3 and in Fig. 10 for HPSN as a function of outer fibre stresses. The results of bending strength measurements are represented in addition, characterized by the mean values and the mean error of mean values. Each plotted mean value corresponds to 6 to 9 single tests.

At short distances between supports, i.e. low compressive stresses, there are deviations from computed curves. Support effects are responsible for this remarkable behaviour, as investigated by

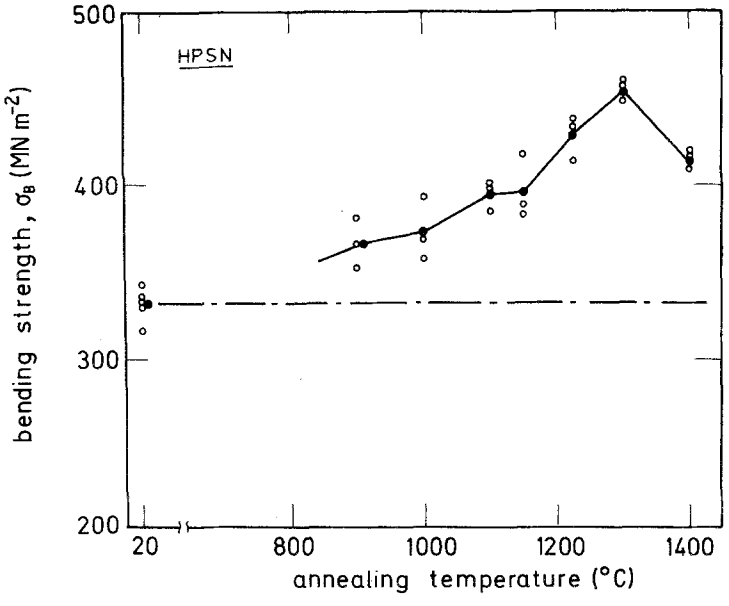

Figure 7 Bending strength of Knoop damaged specimen after 4 h annealing time at various annealing temperatures.

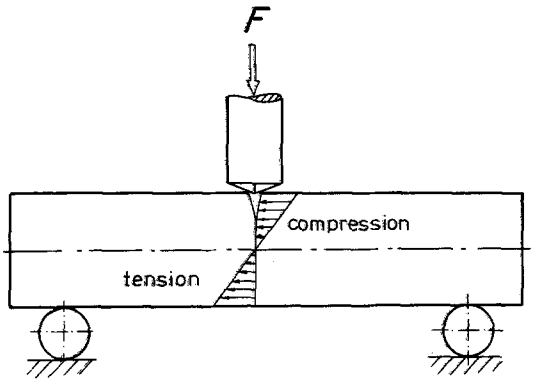

Figure 8 Three-point-bending arrangement for indentation tests on prestressed ceramic surfaces.

Marschall and Rudnick [26] in the 3-point-bending test.

In the left part of Fig. 11 the specimen is supported by a single roller. At the contact line between the roller and specimen a compressive zone exists and acts with forces F/π parallel to the surface. These forces must be balanced by tensile forces in the remaining part of the cross-section. The tensile stresses are approximately

$$\sigma_z \simeq F/\pi bh \tag{44}$$

The compressive zone generates a supplementary bending moment

$$M_b \simeq Fh/2\pi \tag{45}$$

which causes a compressive stress

$$\sigma_b = \frac{M_b}{W} = -\frac{3F}{\pi hb} \quad W = bh^2/6 \tag{46}$$

in the upper surface.

Altogether a compressive stress

$$\sigma \simeq -\frac{2F}{\pi bh} \tag{47}$$

results on the upper surface. With $F = 300\,\mathrm{N}$, $b = 4.5\,\mathrm{mm}$, $h = 3.5\,\mathrm{mm}$ one obtains

$$\sigma \simeq -12\,\mathrm{N\,mm^{-2}} \tag{48}$$

In case of a greater roller distance, this effect vanishes from the range of indentation. The strength values, measured at shorter roller distances, have to be corrected according to Equation 48.

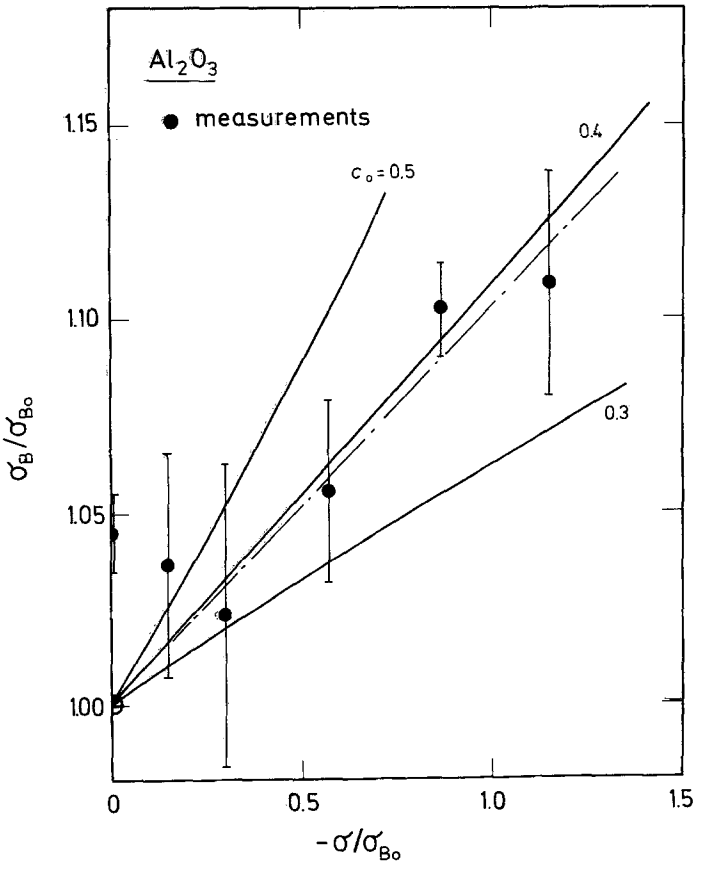

Figure 9 Bending strength of Knoop damaged specimen (Al_2O_3). Knoop indentation tests were carried out with a prestressed specimen.

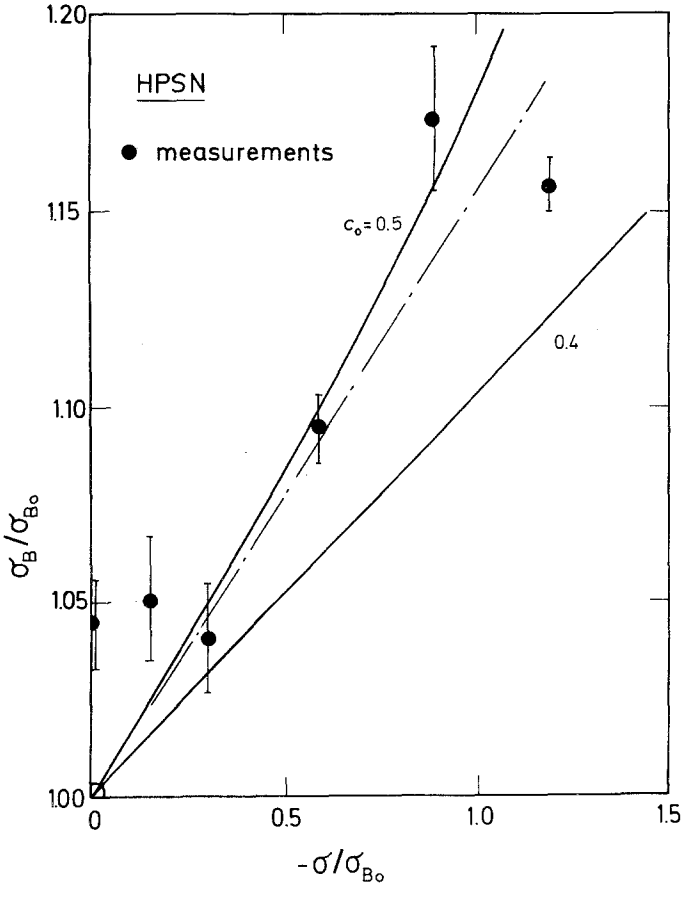

Figure 10 Bending strength of a Knoop damaged specimen (HPSN), analogous to Fig. 9.

From a comparison between measured and calculated curves follows

$$c_0(Al_2O_3) \simeq 0.39$$

$$c_0(HPSN) \simeq 0.48$$

From the bending strength without prestress, reported in Section 4.1, we get

$$\alpha(Al_2O_3) = 0.383$$

$$\alpha(HPSN) = 0.466$$

Except for the support effects, the theoretical curve is in good agreement with the measurement.

By application of these parameters we obtain the results given in Table I

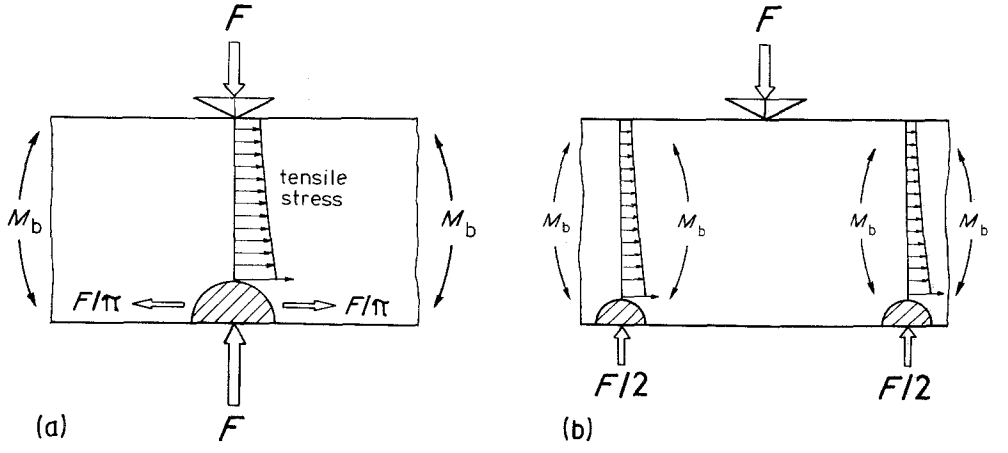

Figure 11 Influence of support effects on the Knoop indentation test.

TABLE I

	Al_2O_3	HPSN
$K_{Fo}/K_c = \alpha$	0.383	(0.466)
K_{Fc}/K_c	0.119	(0.075)
K_{Fc}/K_{Fo}	0.31	(0.16)
R_c/R_0	1.38	(1.64)
F_c'/F_0'	0.51	(0.336)

where $K_{Fo} = K_F^*(R^* = R_0)$ = residual K-value after unloading, and $K_{Fc} = K_F^*(R^* = R_c)$ = residual K-value at failure in the bending test. This shows distinctly that residual wedging decreases with increasing tensile stress in the bending strength test. The data for HPSN are associated with a great uncertainty, since the change in strength after annealing was only interpreted as stress removal.

These results are in contrast to conclusions of Marshall *et al.* [27] obtained from tests with soda-lime glass. From measurements of the mirror/flaw size ratio it was concluded that the residual wedge forces in glass do not relax due to applied tension.

6. Summary

1. The crack opening behaviour of surface flaws, produced by Knoop indentation tests, has been analysed, replacing the damaged region below the indenter tip by a wedge. Computations were performed for a plastically deformable and for a rigid wedge.

2. The residual wedging forces after removal of the Knoop indenter were calculated under the assumption, that the remaining wedge thickness is reduced by a constant factor. So the influence of wedging on bending strength could be analysed.

3. Necessary parameters could be determined by measurements of bending strength of Knoop damaged specimens before and after annealing and by indentation tests in controlled prestressed surfaces.

4. It was found, that the wedging forces were reduced to 40% after removal of indenter. In the following bending tests an additional reduction of about 50% was stated. This relaxation is caused by external stresses and the increase of crack size by stable crack growth.

Acknowledgements

The experimental work was conducted while the author was affiliated with the German Aerospace Research Establishment (DFVLR). The writer thanks G. Himsolt and J. Eschweiler for helpful contributions to the present work and D. Munz, Universität Karlsruhe for stimulating discussions.

References

1. J. J. PETROVIC and L. A. JACOBSON, Proceedings of the Second Army Materials Technology Conference, 1973.
2. J. J. PETROVIC, L. A. JACOBSON, P. K. TALTY and A. K. VASUDEVAN, *J. Amer. Ceram. Soc.* **58** (1975) 113.
3. J. J. PETROVIC, R. A. DIRKS, L. A. JACOBSON and M. G. MENDIRATTA, *ibid.* **59** (1976) 177.
4. R. R. WILLS and J. M. WIMMER, *ibid.* **59** (1976) 437.
5. R. R. WILLS, M. G. MENDIRATTA and J. J. PETROVIC, *J. Mater. Sci.* **11** (1976) 1330.
6. M. V. SWAIN, *ibid.* **11** (1976) 2345.
7. B. R. LAWN and M. V. SWAIN, *ibid.* **10** (1975) 113.
8. G. ZIEGLER and D. MUNZ, *Ber. Deutsch. Ker. Ges.* **56** (1979) 128.
9. G. ZIEGLER and M. MAJDIC, *Beitr. Electronenmikr. Direktabb. Oberfl.* **11** (1978) 137.
10. G. ZIEGLER and D. MUNZ, *Sci. Ceram.* **9** (1977) 502.
11. I. N. SNEDDON, *Proc. Roy. Soc.* **A187** (1946) 229.
12. H. G. HAHN, "Bruchmechanik" (B.G. Teubner, Stuttgart 1976).
13. P. FRANK and R. V. MISES, Die Differential u. Integralgleichungen der Mechanik und Physik Bd. II, Fr. Vieweg, Braunschweig 1961.
14. W. GRÖBNER and N. HOFREITER, Integraltafeln, Teil II, 4. Aufl., Wien (1965).
15. B. R. LAWN and M. V. SWAIN, *J. Mater. Sci.* **10** (1975) 113.
16. B. R. LAWN, S. M. WIEDERHORN and H. H. JOHNSON, *J. Amer. Ceram. Soc.* **58** (1975) 428.
17 B. R. LAWN and R. WILSHAW, *J. Mater. Sci.* **10** (1975) 1049.
18. B. R. LAWN and E. R. FULLER, *ibid.* **10** (1975) 2016.
19. D. B. MARSHALL and B. R. LAWN, *ibid.* **14** (1979) 2001, 2225.
20. P. CHANTIKUL, B. R. LAWN and D. B. MARSHALL, *J. Amer. Ceram. Soc.* **64** (1981) 322.
21. G. R. ANSTIS, P. CHANTIKUL, B. R. LAWN and D. B. MARSHALL, *ibid.* **64** (1981) 533.
22. P. CHANTIKUL, G. R. ANSTIS, B. R. LAWN and D. B. MARSHALL, *ibid.* **64** (1981) 539.
23. G. ZIEGLER, *Ber. Dt. Keram. Ges.* **55** (1978) 397.
24. D. MUNZ, G. HIMSOLT and J. ESCHWEILER, *J. Amer. Ceram. Soc.* **63** (1980) 341.
25. T. FETT, Thesis, University of Karlsruhe, Germany (1983).
26. C. W. MARSCHALL and A. RUDNICK, "Fracture Mechanics of Ceramics" Vol. 1 (Plenum Press, New York, 1974) pp. 69–92.
27 D. B. MARSHALL, B. R. LAWN and J. J. MECHOLSKY, *J. Amer. Ceram. Soc.* **63** (1980) 358.

Received 4 May
and accepted 22 June 1983